

The GDP-bound form of Arf6 is located at the plasma membrane

Eric Macia¹, Frédéric Luton¹, Mariagrazia Partisani¹, Jacqueline Cherfils², Pierre Chardin¹ and Michel Franco^{1,3,*}

¹Institut de Pharmacologie Moléculaire et Cellulaire, CNRS-UMR 6097, 660 route des Lucioles, 06560 Valbonne Sophia-Antipolis, France

²Laboratoire d'Enzymologie et de Biochimie Structurales, CNRS, 1, avenue de la Terrasse, 91198 Gif sur Yvette, France

³Institut de Pharmacologie Moléculaire et Cellulaire, CNRS-UMR 6097, 660 route des Lucioles, 06560 Valbonne-Sophia-Antipolis, France

*Author for correspondence (e-mail: franco@ipmc.cnrs.fr)

Accepted 8 January 2004

Journal of Cell Science 117, 2389-2398 Published by The Company of Biologists 2004

doi:10.1242/jcs.01090

Summary

The function of Arf6 has been investigated largely by using the T27N and the Q67L mutants, which are thought to be blocked in GDP- and GTP-bound states, respectively. However, these mutants have been poorly characterized biochemically. Here, we found that Arf6(T27N) is not an appropriate marker of the inactive GDP-bound form because it has a high tendency to lose its nucleotide *in vitro* and to denature. As a consequence, most of the protein is aggregated *in vivo* and localizes to detergent-insoluble structures. However, a small proportion of Arf6(T27N) is able to form a stable complex with its exchange factor EFA6 at the plasma membrane, accounting for its dominant-negative phenotype. To define the cellular

localization of Arf6-GDP, we designed a new mutant, Arf6(T44N). *In vitro*, this mutant has a 30-fold decreased affinity for GTP. *In vivo*, it is mostly GDP bound and, in contrast to the wild type, does not switch to the active conformation when expressed with EFA6. This GDP-locked mutant is found at the plasma membrane, where it localizes with EFA6 and Ezrin in actin- and phosphatidylinositol (4,5)-bisphosphate-enriched domains. From these results, we conclude that the Arf6 GDP-GTP cycle takes place at the plasma membrane.

Key words: Aggresomes, Arf6, Dominant-negative mutant, Endocytosis, Guanine-nucleotide-exchange factor

Introduction

The ADP-ribosylation factors (Arfs) are small GTP-binding proteins that regulate intracellular vesicular transport along secretory and endocytic pathways. Arf1 and Arf6 are the best-characterized proteins of this six-member family. Arf1 is involved in intra-Golgi transport by recruiting onto membranes the COPI coat that promotes the formation of transport vesicles and the selection of cargo within these vesicles (Chavrier and Goud, 1999; Lanoix et al., 1999). Arf1 is also required for the recruitment of the clathrin-coat adaptor AP1 to the trans-Golgi network (TGN) (Stammes and Rothman, 1993). In addition, Arf1 and Arf6 modulate lipid composition and membrane curvature by activating lipid-modifying enzymes such as phospholipase D (Brown et al., 1993; Cockcroft et al., 1994; Massenburg et al., 1994) and phosphatidylinositol-(4)-phosphate 5-kinase (Aikawa and Martin, 2003; Godi et al., 1999; Honda et al., 1999; Krauss et al., 2003). Arf6 has been implicated in endocytosis and actin rearrangements at the cell periphery (Chavrier and Goud, 1999) but its precise function remains to be discovered. Two mutants of Arf6, Q67L and T27N, are considered to mimic the GTP- and GDP-bound forms, respectively, and have been used extensively to apprehend the localization and the function of the protein. Both immunoelectron microscopy and immunofluorescence (IF) analyses have revealed that the Q67L mutant is restricted to the plasma membrane, whereas the T27N mutant is found on internal structures resembling endosomes (D'Souza-Schorey et al., 1998; Peters et al., 1995; Radhakrishna et al., 1996). Thus,

based on the localization of these two mutants, it has been proposed that Arf6 cycles between the plasma membrane (Arf6-GTP) and a recycling endosomal compartment (Arf6-GDP). In this model, Arf6-GDP would encounter its exchange factor at the surface of an internal compartment to promote the formation of vesicles destined to the plasma membrane. This model has been supported by the observation that expression of the T27N mutant prolonged the accumulation of transferrin inside the cell (D'Souza-Schorey et al., 1995). Also, in HeLa cells, Arf6 has been involved in the recycling of the non-clathrin-dependent internalized interleukin-2 receptor α subunit to the plasma membrane (Radhakrishna and Donaldson, 1997). However, this hypothesis is challenged by other observations. First, by using free-flow electrophoresis in CHO cells, endogenous Arf6 has been found to localize exclusively to the plasma membrane (Cavenagh et al., 1996). Second, in polarized epithelial cells, Arf6 has been found to regulate clathrin-dependent endocytosis of polymeric immunoglobulin A from the apical plasma membrane without affecting its recycling (Altschuler et al., 1999), and to regulate the basolateral endocytosis of E-cadherin (Palacios et al., 2002). Finally, we have cloned and characterized an Arf6-specific exchange factor, EFA6, that is exclusively found at the plasma membrane, implying that Arf6-GDP should also be found at the plasma membrane (Franco et al., 1999).

These different results regarding the localization of the inactive form of Arf6 led us to reconsider the use of the T27N mutant as a marker for Arf6-GDP. The mutation of this

conserved residue in the phosphate-binding P-loop is broadly used to investigate the cellular function of the small G proteins. This mutation generally, but not always, yields a protein with a dominant-negative cellular activity that can be explained biochemically by the formation of a nucleotide-free complex with guanine-nucleotide-exchange factors (GEFs) in which the GEFs are sequestered precluding the activation of their endogenous substrates (Feig, 1999). As well as this activity, G proteins carrying this mutation are often considered to be an approximation of their GDP-bound form and used to determine the localization of the inactive form. However, structural studies show that the Ser/Thr-to-Asn mutation targets a set of interactions that is common to both the GDP- and GTP-bound forms of small G proteins. Thus, their mutant versions are predicted to have impaired interactions with both nucleotides, yielding empty proteins that could trap the GEFs in the cell but not mimic a GDP-bound form.

In this study, we set out to determine the precise localization of Arf6-GDP. In agreement with our prediction, we demonstrate that Arf6(T27N) mutant could not mimic a GDP-bound form. Indeed, this mutation affects the binding of both nucleotides and leads to instability and self-aggregation of Arf6. To investigate the cellular localization of Arf6-GDP, we made a new mutation (T44N) based on the GDP-GTP structural cycle of Arf6 (Menetrey et al., 2000; Pasqualato et al., 2001) that was predicted to lower the affinity for GTP selectively, without affecting that for GDP. We demonstrate that this Arf6(T44N) mutant is locked and stable in the GDP-bound form. It is not found on internal structures but instead at the plasma membrane, where it localizes to discrete sites with the exchange factor EFA6. We conclude that the Arf6 GDP-GTP cycle takes place at the plasma membrane.

Materials and Methods

Cell culture, reagents and antibodies

Baby hamster kidney cells (BHK) were grown in BHK-21 medium (Gibco-BRL), containing 5% fetal calf serum (FCS), 10% tryptose phosphate broth, 100 U ml⁻¹ penicillin, 100 µg ml⁻¹ streptomycin and 2 mM L-glutamine. The following antibodies were used: rat and mouse monoclonal antibodies (mAbs) against hemagglutinin (HA) epitope (clone 3F10 and 12CA5; Roche Diagnostics, Mannheim, Germany), mouse mAb against Myc epitope (clone 9E10), mouse mAb against Tfn-R (clone H68.4; Zymed, CA), rabbit antiserum against Ezrin (provided by M. Martin, CNRS, Montpellier), rabbit antiserum against Arf6 (provided by V. Hsu, Harvard Medical School, Boston, MA), mouse mAb against Arf6 (provided by S. Bourgoin, Sainte-Foy, Quebec, Canada), mouse mAb against Giantin (provided by H-P. Hauri, Basel, Switzerland), mouse monoclonal anti vimentin (clone V9; Sigma). Texas-Red conjugated phalloidin and Texas-Red-conjugated wheat-germ agglutinin (WGA) were from Molecular Probes, FITC and Texas-Red-conjugated antibodies were from Jackson ImmunoResearch. Azolectin and unlabelled nucleotides were from Sigma Chemical (St Louis, MO). [³²P]-Orthophosphate, [³H]-GDP and [¹²⁵I] were from Amersham Pharmacia Biotech (Uppsala, Sweden) and [³⁵S]-GTPγS from NEN-Perkin Elmer. Nocodazol was from Calbiochem (Merk Eurolab, France).

Preparation of phospholipid vesicles

Large unilamellar vesicles of azolectin were prepared as described elsewhere (Szoka and Papahadjopoulos, 1978) and were extruded

through a 0.1 µm pore size polycarbonate filter (Isopore; Millipore). Vesicles of defined composition were prepared as previously described (Macia et al., 2000).

Expression and purification of recombinant proteins

Myristoylated ARF6 wild type (myrARF6-wt) and mutants were expressed and purified as previously described (Chavrier and Franco, 2001; Franco et al., 1995a). The myrARF6-wt and Q67L mutant proteins were essentially purified as GTP-bound forms, whereas myrARF6(T44N) and T27N were purified in the GDP-bound form. EFA6 was purified as previously described (Macia et al., 2001).

Fluorescence measurements

The large increase in intrinsic fluorescence of ARF-GTP over ARF-GDP (Kahn and Gilman, 1986) was used to monitor in real time ARF6 activation upon GDP to GTP exchange and ARF6 deactivation after GTP hydrolysis. All measurements were performed in HKM buffer (50 mM Hepes, pH 7.5, 100 mM KCl, 1 mM MgCl₂, 1 mM DTT) supplemented with azolectin vesicles (final lipid concentration 0.4 g l⁻¹) at 37°C unless otherwise indicated.

GDP or GTPγS dissociation assay

The GDP or GTPγS dissociation assay was performed essentially as described before (Franco et al., 1996; Macia et al., 2001). Briefly, myrARF proteins (~10 µM) were first loaded with [³H]-GDP (150 µM, 1000 cpm pmol⁻¹) or [³⁵S]-GTPγS (1000 cpm pmol⁻¹) by incubating them for 45 minutes at 37°C in HKM buffer containing 1 µM free Mg²⁺ (1 mM MgCl₂ and 2 mM EDTA). When maximal loading was reached, the concentration of free Mg²⁺ was raised to 1 mM to stop the reaction. This solution was diluted ten times (1 µM final) in HKM buffer supplemented with lipid vesicles, and nucleotide dissociation was monitored as a loss of protein-bound radiolabel following addition of 1 mM unlabeled nucleotide.

Sedimentation analysis of the stability of Arf6(T27N) and Arf6(T44N) mutants

Myristoylated purified Arf6(T27N) or Arf6(T44N) (~5 µM) was incubated with 50 µM GDP in 50 mM Tris HCl, pH 8.0, 1 mM MgCl₂ and 0.5 mM DTT. After a 2-hour incubation at 37°C, the 200 µl sample was ultracentrifuged (in a Beckman TLA 100.1 rotor) for 30 minutes at 50,000 g. The supernatant and the pellet which has been resuspended with 200 µl of the same buffer, were analysed by Coomassie-Blue-stained SDS-PAGE and densitometry.

Cell fractionation, Triton X-100 solubilization and immunoblotting

10⁶ BHK cells were transfected with Arf6-expressing vectors and, 40 hours later, the cells were washed in PBS. For cytosol-membrane fractionation, the cells were homogenized in 250 mM sucrose, 3 mM imidazole, pH 7.4, with protease inhibitors. The post-nuclear supernatant (PNS) was obtained by centrifugation of the cell lysate at 1000 g for 5 minutes at 4°C. The PNS was further centrifuged for 45 minutes at 100,000 g to separate the membrane and cytosolic fractions. For Triton X-100 solubilization, the cells were lysed in 20 mM Tris-HCl, pH 7.5, 1% Triton X-100, 120 mM NaCl, 1 mM MgCl₂ and protease inhibitors for 10 minutes at 4°C, and centrifuged for 30 minutes at 15,000 g to separate Triton-X-100-soluble from -insoluble fractions. Aliquots of the pellet and supernatant (one-sixth of the pellet for the Triton-X-100-solubilization experiment) fractions were loaded on a 15% sodium-dodecyl-sulfate (SDS) polyacrylamide gel and analysed by immunoblot using anti-HA antibodies to detect ARF6.

Co-immunoprecipitation

BHK-21 cells (2×10^6 cells in 100 mm tissue culture dishes) were transfected or not (mock) with mycArf6T27N or EGFP-EFA6 constructs or both. 48 hours after transfection, cells were lysed in 0.5 ml of lysis buffer [20 mM Hepes, pH 7.4, 1% NP-40, 100 mM NaCl, 1 mM MgCl₂, 0.25 mM PMSF and a tablet of protease inhibitors (Roche)]. Lysates were clarified by centrifugation at 13,000 *g* for 30 minutes, aliquots of each supernatants were kept for analysis. Then 5 µg of 9E10 antibody and 20 µl protein-A/Sepharose-CL4B were added for 4 hours at 4°C. The beads were then washed in lysis buffer and immunoprecipitated proteins were separated by 15-10% SDS-polyacrylamide-gel electrophoresis (SDS-PAGE) and transferred to nitrocellulose membranes.

Determination of the GDP/GTP ratio

BHK cells were seeded in 100 mm tissue culture dishes at 2×10^6 cells per dish. The following day, the cells were transfected with the various Myc-tagged Arf6 constructs alone or in combination with a plasmid encoding EGFP-EFA6 using the Fugene 6 transfection reagent according to the manufacturer instructions (Roche Diagnostics, Mannheim). 32 hours after transfection, the cells were transferred to phosphate-free and serum-free Dulbecco's modified Eagle's medium (ICN, Costa Mesa, California) supplemented with 0.25 mCi ml⁻¹ [³²P]-orthophosphate for 16 hours. The cells were washed three times with cold PBS and then lysed in lysis buffer [20 mM Hepes, pH 7.4, 1% NP-40, 100 mM NaCl, 1 mM MgCl₂, 0.25 mM PMSF and a tablet of protease inhibitors (Roche)]. After centrifugation at 15,000 *g* for 30 minutes, the supernatant was subjected to immunoprecipitation with 5 µl of 9E10 ascites fluid and 20 µl protein-A/Sepharose-CL4B for 2 hours at 4°C. The beads were then washed five times in lysis buffer. 20 µl of elution buffer (75 mM KH₂PO₄, pH 3.4, 5 mM EDTA, 0.1% SDS, 1.5 mM GDP, 1.5 mM GTP) was added to the beads and the mixture was heated to 85°C for 3 minutes. After centrifugation (15,000 *g*, 2 minutes) 5 µl of supernatants were spotted onto polyethyleneimine (PEI)-cellulose thin-layer chromatography plates (Merck), which were developed for 2 hours in 0.65 M KH₂PO₄, pH 3.4. After autoradiography, separated guanine nucleotides were visualized with ultraviolet light, cut from the chromatography plates and the radioactivity was quantified by counting in β-radiation counter (Beckman).

Pull-down assay for Arf6-GTP

Activation levels of expressed Arf6 proteins were assayed essentially as described by Niedergang et al. (Niedergang et al., 2003). Briefly, 24 hours after transfection, BHK cells (5×10^6 per condition) were lysed at 4°C in 1 ml lysis buffer (50 mM Tris HCl, pH 8.0, 100 mM

NaCl, 10 mM MgCl₂, 1% Triton X-100, 0.05% sodium cholate, 0.005% SDS, 10% glycerol, 2 mM DTT with protease inhibitors). Lysates were clarified by centrifugation at 13,000 *g* for 10 minutes and incubated with 0.5% bovine serum albumin and 40 µg GST-GGA₃(1-226) bound to glutathione-Sepharose beads (Amersham Pharmacia Biotech) for 40 minutes. The beads were washed three times in lysis buffer and bound proteins eluted in 30 µl SDS-PAGE sample buffer. Normalized amounts of total Arf6 from the starting lysates were loaded on the gel and assessed for the presence of Arf6-GTP by western blot using an anti-Arf6 antibody.

Confocal immunofluorescence microscopy

BHK cells plated on 11 mm round glass coverslips were transiently transfected with pCDNA3 or pEGFP-N1/C1 constructs using the Fugene 6 transfection reagent as described by the manufacturer (Roche). Unless otherwise stated, the cells were washed twice in PBS 24 hours after transfection, then fixed in 3% paraformaldehyde and processed for IF analysis as described previously (Franco et al., 1998). For vimentin labelling, cells were fixed at -20°C for 4 minutes in methanol followed by 30 seconds in acetone. For surface staining, cells were incubated for 2 minutes on ice with 0.5 µg ml⁻¹ Texas-Red-conjugated WGA before fixation. Confocal microscopy analysis was carried out with a Leica TCS-SP microscope equipped with a mixed-gas argon/krypton laser (Leica Microsystems).

Results

Structural analysis of the roles of Thr27 and Thr44 residues in Arf6 nucleotide binding

Thr27 is a conserved residue in the P-loop that interacts with the β-phosphate of the nucleotide and the magnesium ion in both conformations (Fig. 1). We thus predicted that the Thr27 mutation would result in a lowered affinity for both nucleotides. We looked for an alternative mutation that would only decrease GTP binding, without affecting the affinity for GDP. Arf6, like other members of the Arf family, features a unique nucleotide conformational switch, one aspect of which is the rearrangement of the switch-1 region (Pasqualato et al., 2002). Unlike Ras, Rho and Rab proteins, switch 1 in Arf-GDP forms an extra β-strand remote from the GDP nucleotide, and undergoes a large rearrangement upon binding of GTP that restores a nucleotide binding site similar to that of other families of small GTP-binding proteins (Fig. 1). Thus, residues in switch 1 that interact with GTP make excellent candidates for designing Arf mutants trapped in the GDP-bound form. We

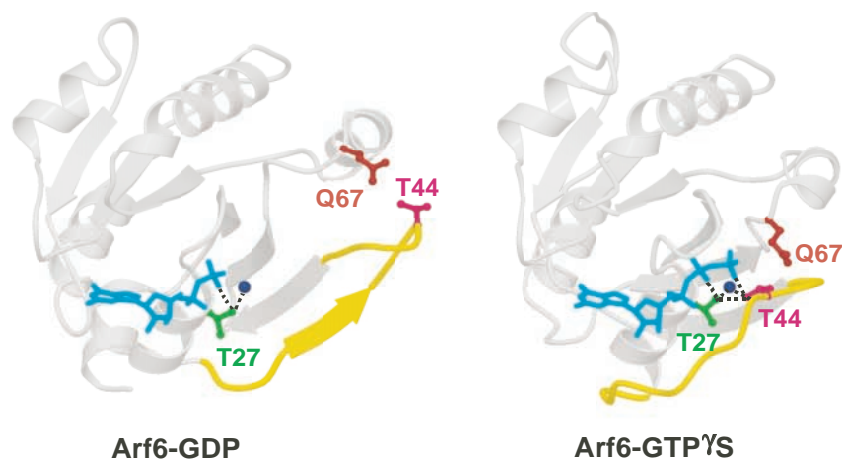


Fig. 1. Representation of the structural positions of the Thr27, Thr44 and Gln67 residues of Arf6 in both GDP and GTP conformations based on crystallographic studies of Arf6-GDP (PDB entry 1EOS) (Menetrey et al., 2000) and Arf6-GTPγS (PDB entry 1HFV) (Pasqualato et al., 2001). Thr27 residue (in green) is involved in the binding of the magnesium ion (in copper) and the β phosphate of the two nucleotides. Gln67 (in brown) from the switch II region and Thr44 (in purple) from the switch I region undergo a large conformational change between the two states that repositions them near the γ phosphate in the GTP state. Thr44 is involved in the binding of the γ phosphate and the magnesium ion.

selected Thr44, an invariant residue of small GTP-binding proteins, because it is exposed to the solvent in Arf6-GDP, whereas it interacts with the γ -phosphate, Mg^{2+} and Thr27 in the P-loop in Arf6-GTP (Fig. 1). We thus predicted that replacement of Thr44 by a bulkier residue would result in the inability of switch 1 to adopt a GTP-bound conformation without affecting its conformation in Arf6-GDP. In consequence, the improper coordination of GTP by the mutant would effectively trap the protein in the GDP-bound form. In fact, it has been previously reported that the mutation of the equivalent residue in Rap2 protein (Thr 35) resulted in a decreased affinity for GTP without affecting GDP binding (Lerosey et al., 1991).

In vitro, the T27N mutation affects both GDP and GTP binding, whereas the T44N mutation affects solely GTP binding

We purified from bacteria the myristoylated proteins wild-type Arf6, Arf6(T27N) and Arf6(T44N). It is noteworthy that Arf6-wt is produced by the bacteria as a GTP-bound form, whereas Arf6(T44N) is found essentially associated with GDP. The purification of Arf6(T27N) could only be achieved in the presence of a large excess of GDP (0.1 mM) in all buffers to prevent its denaturation and sedimentation during the centrifugations.

The effect of the T27N mutation on the GDP dissociation rate was analysed in vitro at physiological Mg^{2+} concentration in the presence of phospholipids (Fig. 2A). Myristoylated Arf6 proteins (mutant and wild type) were first loaded with [3H]-GDP; GDP dissociation was then measured after addition of an excess of unlabelled GDP. We observed that the T27N mutation increased the GDP off-rate nearly fivefold compared with Arf6-wt. We conclude that the mutation of Thr27 results in a lower affinity for GDP. We tried to determine the impact of the mutation on the affinity for GTP but we could not find any experimental conditions enabling us to load the T27N mutant with [^{35}S]-GTP γ S. This observation indicates that the T27N mutation dramatically decreases the affinity for GTP. The fact that the T27N substitution decreases the affinity of the protein for the nucleotides raises the question of its stability in solution. This was assessed directly by looking at the stability of the association between the nucleotide and the protein. Arf6(T27N) was first loaded with [3H]-GDP at low Mg^{2+} concentration to accelerate nucleotide exchange. When maximal loading was attained, the Mg^{2+} was raised up to physiological concentration (1 mM) and the radioactivity bound to the proteins monitored as a function of time. After a 1-hour incubation at 37°C, more than 50% of Arf6(T27N) had lost its nucleotide (Fig. 2C). The stability of Arf6(T27N) was also investigated in a sedimentation experiment. After a 2-hour incubation at 37°C, about half of the protein was found in the pellet (Fig. 2D). Altogether, these results indicate that the T27N mutant is unstable and has a high tendency to lose its nucleotide.

When the T44N mutant was examined for its nucleotide-binding properties, we first observed that its GDP off-rate was unchanged and similar to that of Arf6-wt (Fig. 2A). Second, we found that the GTP off-rate was about 30-fold higher than for the wild-type protein (Fig. 2B). From these experiments, we conclude that the Thr44 residue does not participate in the binding of GDP but is strongly implicated in the interaction

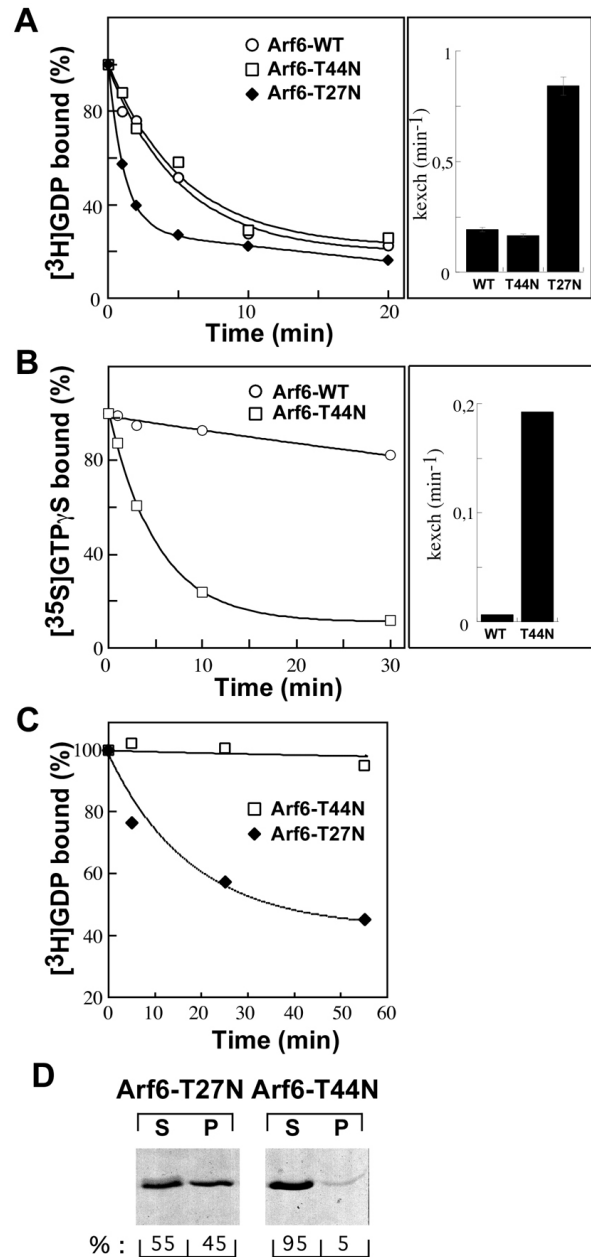


Fig. 2. T27N mutation decreases the affinity of Arf6 for both GDP and GTP γ S and destabilizes the protein. T44N mutation affects the binding of GTP γ S but not of GDP. (A,B) Arf6 wt (○), Arf6-T27N (◆) or Arf6-T44N (□) were loaded for 40 minutes at 37°C with [3H]-GDP (A) or [^{35}S]-GTP γ S (B) in the presence of 1 μ M free Mg^{2+} . Then, the free Mg^{2+} concentration was raised to 1 mM and [3H]-GDP and [^{35}S]-GTP γ S dissociations were initiated by adding 1 mM unlabeled GDP or GTP γ S, respectively. The curves are best fits assuming first-order kinetics for nucleotide dissociation; nucleotide dissociation rates are shown on the left. (C) Arf6 T27N (◆) or T44N (□) were loaded at 37°C with [3H]-GDP in the presence of 1 μ M free Mg^{2+} . Then, the free Mg^{2+} concentration was raised to 1 mM and, without isotopic dilution, the radioactivity bound to the proteins was measured over time. (D) Arf6-T27N or Arf6-T44N (5 μ M) was incubated in the presence of 50 μ M GDP and 1 mM free Mg^{2+} for 2 hours at 37°C. After ultracentrifugation, pellet (P) and supernatant (S) were analysed by SDS-PAGE and Coomassie Blue staining. The distribution (as percentages) of Arf between pellet and supernatant is indicated.

between Arf6 and the γ -phosphate of the GTP. Third, we determined that the T44N mutant was stable in solution, because more than 95% of the protein was still soluble (Fig. 2D) and associated to its nucleotide GDP after a 1-hour incubation at 37°C (Fig. 2C). Therefore, Arf6(T44N), in contrast to Arf6(T27N), is a stable GDP-bound protein.

Expression of Arf6(T27N) leads to the formation of aggregated structures reminiscent of aggresomes

Our *in vitro* data demonstrate that Arf6(T27N) is an unstable protein that easily loses its nucleotide leading to its denaturation. We therefore analysed its behaviour when expressed in cells. We compared the distribution of the different Arf6 proteins following cytosol-membrane fractionation of transfected BHK cells. Overexpressed Arf6-wt distributes almost equally between pellet and soluble fractions (Fig. 3A). Arf6(T44N) displays a very similar distribution. As for Q67L and T27N mutants, both are essentially in the pellet. However, when transfected BHK cells were lysed in the presence of Triton X-100, a nonionic detergent used to solubilize the membranes at 4°C, Arf6(T27N) was still found in the pellet, whereas Arf6-wt and the two other mutants were solubilized and mostly recovered in the supernatant (Fig. 3B). We noticed that Arf6(T27N) was still Triton X-100 insoluble when the cells were treated with cytochalasin D, suggesting that Arf6(T27N) is not associated with the actin cytoskeleton (data not shown). It has been reported recently that misfolded and aggregated proteins could be intracellularly sequestered

into specialized structures named aggresomes (Garcia-Mata, 2002). These structures are Triton X-100 insoluble and formed by the condensation of mini-aggregates, transported and regrouped in a microtubule-dependent manner in a perinuclear region, probably the microtubule organizing centre. In some cases, the presence of aggresomes induces the formation of a vimentin cage surrounding the aggregates. In agreement with previous studies (Peters et al., 1995; Radhakrishna et al., 1996), using a GFP-coupled Arf6(T27N) protein expressed in BHK cells, we located the mutant predominantly in intracellular dots dispersed throughout the cells. Interestingly, these dots became larger and more concentrated around the nucleus over time (Fig. 3Ca-c). In addition, a 2-hour incubation with nocodazole induced the redistribution and dispersion of these juxtannuclear Arf6(T27N)-positive structures (Fig. 3Cd). Similar observations were made when Arf6(T27N) was HA-tagged and expressed in HeLa and CHO cells (data not shown). At high levels of expression, we observed that Arf6(T27N) perturbed the vimentin cytoskeleton, leading to the formation of a ring around the Arf6(T27N)-labelled structures (Fig. 3Ce-g).

Altogether, these results indicate that cellular expression of Arf6(T27N) leads to the formation of structures reminiscent of aggresomes. We conclude that the T27N mutant should not be used to determine the cellular localization of the GDP-bound form of Arf6.

Arf6(T27N) inhibits *in vitro* activation of Arf6-wt by its exchange factor EFA6

However, several studies have shown that, *in vivo*, the expression of Arf6(T27N) mutant could affect Arf6 function. We suspected that this mutant, which has impaired interaction with nucleotides (Fig. 1) could be stabilized by the formation of a nucleotide-free complex with the GEF. Thus, the T27N mutant would sequester the GEF, inhibiting the activation of endogenous Arf6. To demonstrate such a dominant-negative effect, we have tested the ability of Arf6(T27N) *in vitro* to

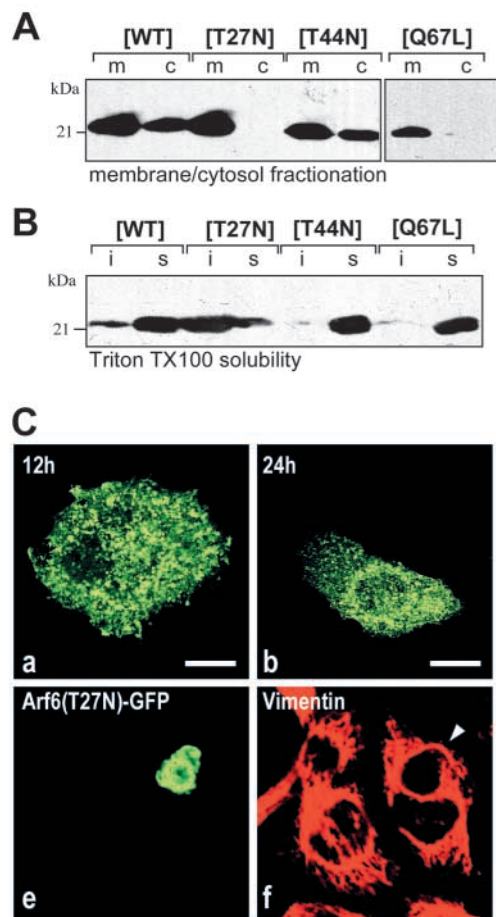


Fig. 3. Arf6(T27N) localizes to detergent-insoluble structures reminiscent of aggresomes. (A,B) When expressed in cells, Arf6(T27N) is essentially insoluble even in the presence of detergent. Cells were transfected with expression plasmids encoding HA-tagged Arf6-wt and the T27N, T44N and Q67L mutants. (A) The cells were homogenized and the post-nuclear supernatants were centrifuged at 100,000 *g* to give a membrane (m) and a cytosolic (c) fraction. (B) BHK-21 cells were lysed at 4°C in Triton-X-100-containing buffer and centrifuged to separate Triton-X-100-soluble (s) and -insoluble (i) fractions. The different fractions were immunoblotted using anti-HA mouse monoclonal antibody. (C) Expression of Arf6(T27N)-EGFP induces the formation of punctate structures that are regrouped near the nucleus over time in a microtubule-dependent

manner. BHK-21 cells were transfected with Arf6(T27N)-EGFP constructs and fixed at different time points. Cells were treated for 2 hours with 30 μ M nocodazole before fixation (d). 48 hours after transfection, cells were probed with anti-vimentin antibodies (e-g). At high expression levels, perinuclear Arf6(T27N)-EGFP structures (e) are surrounded with a vimentin ring (f, arrowheads). A merged image is presented (g).

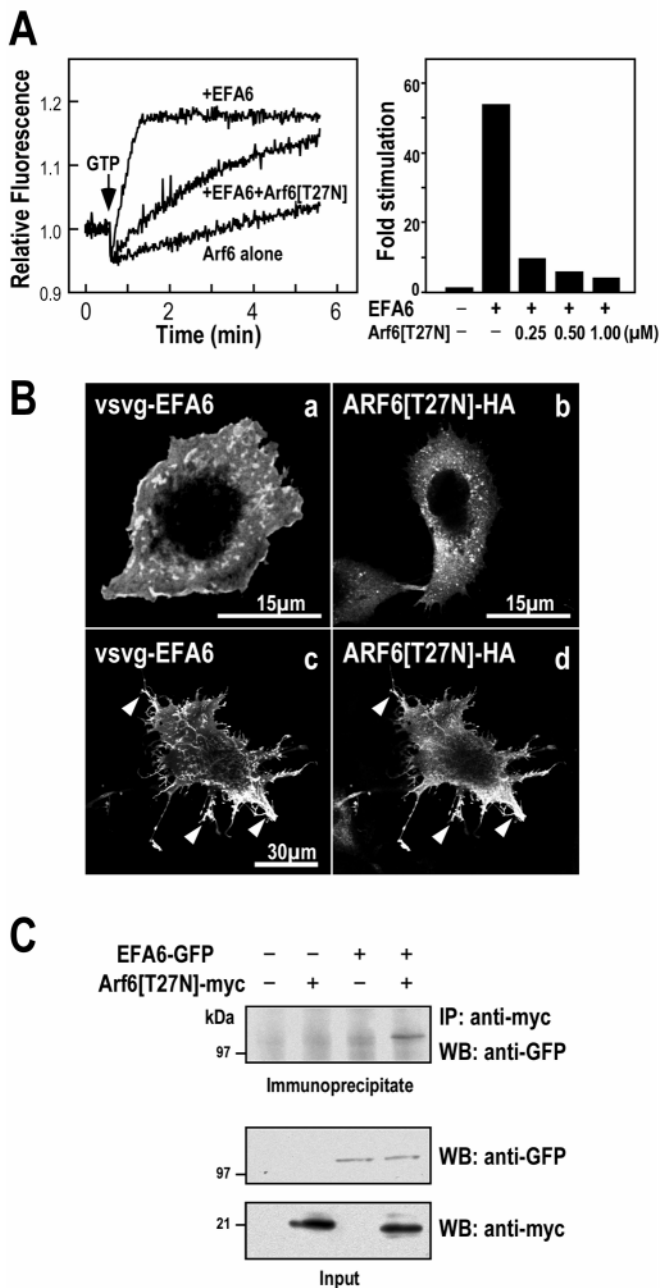
inhibit the activation of Arf6-wt by the specific exchange factor EFA6. As previously shown (Macia et al., 2001), addition of purified EFA6 to GDP-bound Arf6-wt strongly increased the GDP-GTP exchange rate as monitored in real time by tryptophan fluorescence (Fig. 4A). The addition of purified Arf6(T27N) inhibited in a dose-dependent manner the EFA6-catalysed activation of Arf6-wt (Fig. 4A) but had no effect on spontaneous exchange (not shown). From these results, we conclude that, in vitro, the Arf6(T27N) mutant, not yet denatured, can inhibit the activation of Arf6-wt by its GEF.

EFA6 expression redistributes Arf6(T27N) to the cell surface together with EFA6

Next, we tested whether Arf6(T27N) could act in vivo as a dominant-negative protein by forming a stable complex with

EFA6. After co-expression in BHK cells, we examined the localization of the two proteins. As previously reported (Franco et al., 1999), their co-expression induced many long, thin extensions of the plasma membrane. Interestingly, Arf6(T27N) no longer appeared in large intracellular structures but was redistributed together with EFA6 to the cell surface where they colocalized (Fig. 4Bc,d). Co-immunoprecipitation experiment demonstrates that, in vivo, the two proteins are associated (Fig. 4C). This result indicates that the two molecules form a complex by which EFA6 prevents the denaturation and the accumulation of Arf6(T27N) in aggresomes.

Altogether, these results demonstrate for the first time that the Arf6(T27N) mutant acts both in vivo and in vitro as a dominant-negative form by sequestering the exchange factor. In addition, it suggests that, because the complex is found at the plasma membrane, this is where the activation of Arf6 occurs.



In vivo, the Arf6(T44N) mutant is locked in the inactive conformation

Our results demonstrate that, in vivo, a proportion of the Arf6(T27N) mutant is engaged in a high-affinity nucleotide-free complex with the exchange factor, whereas most denatures and accumulates into aggresomes. Thus, the Arf6(T27N) mutant cannot be used to localize the inactive GDP-bound form of Arf6. Our in vitro experiments (Fig. 2) indicated that the Arf6(T44N) mutant would better mimic the inactive form. We verified in vivo that Arf6(T44N) is GDP bound. BHK cells transfected with the Arf6 constructs were radiolabelled with [³²P]-orthophosphate. The Arf6 proteins were immunoprecipitated and the associated nucleotide was analysed by thin-layer chromatography. We observed that the T44N mutant, like the wild-type protein, was essentially GDP bound. Interestingly, when the exchange factor EFA6 was co-

Fig. 4. Arf6(T27N) acts as a dominant-negative mutant both in vitro and in vivo by trapping the exchange factor EFA6. (A) In vitro Arf6(T27N) inhibits EFA6-catalysed activation of Arf6-wt. Kinetics of GDP to GTP exchange on Arf6 were monitored by the correlated variation in tryptophan fluorescence. Purified Arf6 was preloaded with GDP and injected at 0.5 μM in the fluorescence cuvette containing azolectin vesicles (0.4 g l⁻¹) in HKM buffer at 30°C. When indicated, purified EFA6 (100 nM) and increasing concentration of Arf6(T27N) (0–1 μM) were injected, followed by the addition of GTP (200 μM). For better clarity, we have only represented the curve at 1 μM of Arf6(T27N). For each experiments the value of the fold stimulation is plotted. The fold stimulation is the ratio of the EFA6-catalysed over the spontaneous exchange rate. (B) Co-expression with VSV-G-EFA6 induces the redistribution of Arf6(T27N) to the plasma membrane. BHK-21 cells were transfected with VSV-G-EFA6 (a) or Arf6(T27N)-HA (b) or both (c,d). After fixation, the cells were probed with anti-VSV-G antibody to detect EFA6 (a,c) and with anti-HA antibody to detect Arf6 (b,d). The co-expression of Arf6(T27N) and EFA6 induces plasma membrane extensions where they colocalize. Arrows indicate some zones of costaining. (C) EFA6 co-immunoprecipitates with Arf6(T27N). Lysates of BHK-21 cells untransfected or transiently expressing Arf6(T27N)-Myc, EGFP-EFA6 or both were immunoprecipitated (IP) with an anti-Myc antibody. Immunoprecipitates were resolved on SDS-PAGE, blotted on nitrocellulose membranes and probed with an anti-GFP antibody to detect EGFP-EFA6. 5% of the input (cell lysates) was also immunoblotted with anti-GFP and anti-Myc antibodies to ensure that EGFP-EFA6 and Arf6(T27N) respectively were expressed.

transfected, no significant GTP binding was observed on Arf6(T44N) protein, in contrast to the wild-type (Fig. 5A). This result was confirmed in a pull-down assay using the Arf/GTP-binding domain of GGA₃ fused to GST protein (Niedergang et al., 2003). In the absence of expression of EFA6, only Arf6(Q67L) was able to bind to GST-GGA₃ (Fig. 5B). When EFA6 was co-expressed, Arf6-wt bound to GST-GGA₃, whereas Arf6(T44N) did not. We conclude that, in vivo, the T44N mutant is locked in the inactive conformation.

Arf6-GDP accumulates in actin, ezrin and phosphatidylinositol (4,5)-bisphosphate (PIP₂)-enriched structures of the plasma membrane

After having demonstrated that the Arf6(T44N) mutant mimics

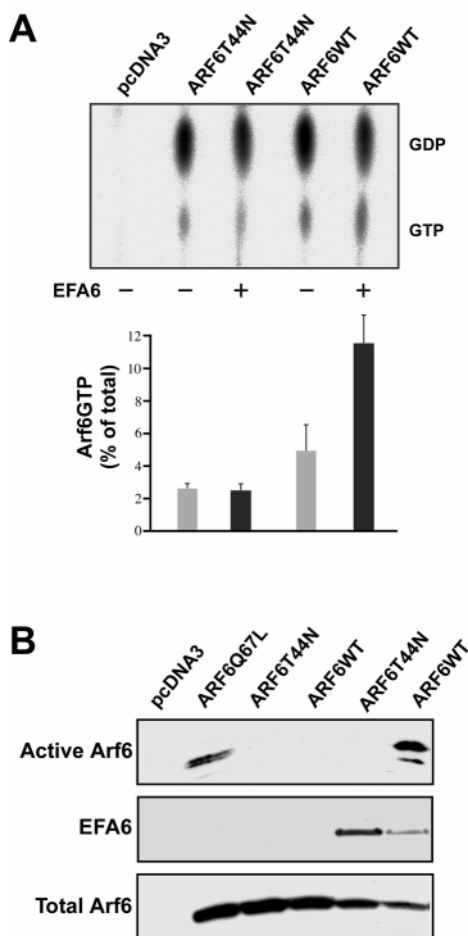


Fig. 5. In vivo, expression of EFA6 leads to the activation of Arf6-wt but not of Arf6(T44N). (A) BHK-21 cells were transfected with expression plasmids encoding Myc-tagged Arf6-wt, or Arf6(T44N) alone or in combination with a plasmid encoding EGFP-EFA6 and grown in the presence of [³²P]-orthophosphate. After immunoprecipitation with the anti-Myc monoclonal antibody, the bound nucleotides were determined by thin-layer chromatography and subjected to autoradiography. The position of GDP and GTP are indicated. (bottom) Quantification of the results from two independent experiments (mean ± SD). (B) BHK-21 cells were transfected with different Arf6 constructs alone or in combination with EGFP-EFA6. Arf6-GTP was isolated by incubation with a GST fusion containing an ARF6 effector domain.

the Arf6 GDP-bound form, we set out to determine the cellular localization of the membrane-associated fraction by confocal IF microscopy. First, Arf6(T44N) was co-transfected with Rab5 or Rab7, markers for early and late endosomes, respectively (Gruenberg, 2001). We did not find any significant co-staining between Arf6(T44N) and these two endosomal proteins (Fig. 6). Arf6(T44N) was also absent from the Tfn-R-positive recycling compartment. However, both proteins were frequently colocalized at the cell surface (Fig. 6). Interestingly, the Arf6(T44N) present at the plasma membrane stained using fluorescent WGA, was also observed in areas devoid of clathrin (Fig. 6). These results suggest that Arf6 is probably not involved in the formation of recycling vesicles from the recycling compartment but might participate at a stage of the Tfn-R endocytosis that precedes its incorporation into clathrin-coated pits.

In addition to its role in endocytosis, Arf6 stimulates the cortical actin rearrangement. Confocal sectioning through the upper part of the cell revealed that Arf6(T44N) localized with F-actin in many cell surface structures, such as large membrane folds and small membrane extensions (Fig. 6). It should be realized that Arf6 is never detected at the ventral cell surface facing the substratum. Ezrin belongs to the ERM protein family, which serve as cytoskeleton-membrane linkers. We compared the distribution of ezrin to Arf6(T44N) and found that both are highly enriched and are remarkably colocalized in the same membrane structures (Fig. 6). Several studies suggest that ezrin could bind selectively to PIP₂ (Barret et al., 2000; Niggli et al., 1995), we asked whether these membrane domains were enriched in specific lipid species. We examined the cellular distribution of PIP₂ by monitoring the PH domain of the PLCδ, which has a high affinity for PIP₂. Cells co-transfected with plasmids encoding PLCδ-PH-GFP and Arf6(T44N) exhibited a strong co-localization of the two proteins at the cell surface confined within the microvilli and large domain folds described above (Fig. 6). We also noticed that PLCδ-PH-GFP labelling was not modified by the expression of Arf6(T44N), suggesting that (as expected) this inactive Arf6 mutant did not affect the phosphatidylinositol-(4)-phosphate 5-kinase activity (not shown). The PH domain of EFA6 being entirely responsible for its plasma membrane attachment (Derrien et al., 2002; Franco et al., 1999), we used an EFA6-PH-GFP construct to compare EFA6 and Arf6(T44N) localizations. We observed that both proteins accumulated in the same areas at the cell surface, indicating that Arf6 and its exchange factor EFA6 encounter one another in discrete plasma membrane domains enriched in cortical actin, ezrin and PIP₂.

Discussion

Mutations of conserved residues in the nucleotide binding site of small GTP-binding proteins that trap or alter specific steps along their GDP-GTP cycle have proved to be invaluable tools to investigate their cellular functions. One of the most popular mutations involves the replacement of a conserved Ser/Thr residue in the phosphate-binding P-loop by an Asn (Thr27 in Arf6), which results in the improper coordination of the β-phosphate of nucleotides and the associated Mg²⁺ ion, and thereby a lowered affinity for GDP and GTP. However, G proteins with this mutation are often called 'GTP-binding-

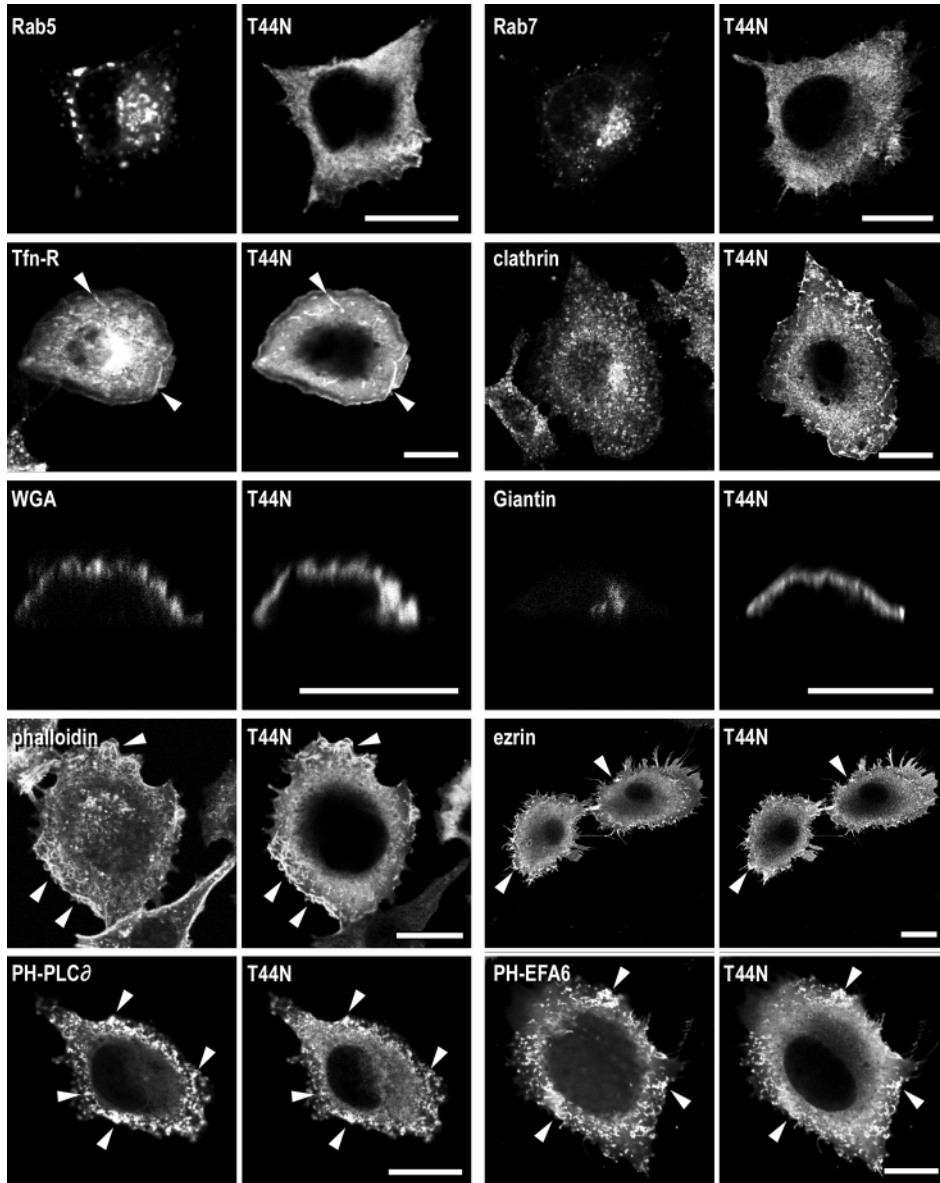


Fig. 6. Arf6-GDP localizes with EFA6 and ezrin in actin- and PIP₂-enriched structures of the plasma membrane. BHK-21 cells were transfected with Arf6(T44N)-HA alone or with GFP-Rab5, GFP-Rab7, PH-PLC δ -GFP or PH-EFA6-GFP. After fixation, the cells were probed with anti-HA antibody to detect Arf6, in combination with phalloidin, anti-Giantin, anti-ezrin, anti-Tfn-R or anti-clathrin-heavy-chain antibodies and analysed by *xy* or *xz* (for WGA and anti-Giantin labelling) confocal sectioning. The cell surface was stained using Texas-red-conjugated WGA. Arrows indicate some zones of co-staining. Scale bars, 15 μ m.

defective mutants' and considered to be an approximation of their GDP-bound state. Here, we have analysed both in vitro and in vivo the impact of this mutation on Arf6. We demonstrated that Arf6(T27N) mutant cannot be used to mimic the GDP-bound form. However, the mutant is particularly well suited to inhibiting endogenous Arf6 activation by trapping the exchange factor.

We observed that the T27N mutation decreased the affinity of Arf6 for both GDP and GTP leading to the occurrence of a nucleotide-free and hence unstable protein. It has been known for the past decade that removing the nucleotide from a G-protein in vitro leads to a so-called 'comatose' protein (Ferguson and Higashijima, 1991). As a consequence, the T27N mutant forms aggregates both in vitro and inside the cell. In vivo, the T27N mutant is essentially localized in non-ionic detergent insoluble structures that are characteristic of aggresomes (Johnston et al., 1998). The formation of aggresome in a juxtannuclear region is proposed to be a general

cellular response to the presence of aggregated and undegraded proteins. We propose that at least a proportion of the perinuclear localized Arf6(T27N) represents aggresomes mistaken for the perinuclear recycling compartment. The instability of the dominant-negative form of ARF6 could be a phenomenon general to the other small G-proteins designed on the same model. Hence, the intracellular localization of these mutants should be interpreted with caution.

However, we found that Arf6(T27N) could still act as a dominant-negative protein. A general feature of GEF catalytic mechanisms is the formation of a G-protein/GEF complex with low affinity for nucleotide. For example, in vitro and in the absence of nucleotide, there is formation of a stable nucleotide-free complex between Arf1 and the isolated Sec7 domain of Arno or Gea2. This complex is disrupted by the addition of nucleotide (Paris et al., 1997; Goldberg, 1998). The lowered affinity of the T27N mutant for both nucleotides explains the formation of a complex between Arf6(T27N) and EFA6 even

in the presence of nucleotide in the medium. In addition, our immunolocalization and co-immunoprecipitation analyses demonstrate that a dominant-negative mutant traps its exchange factor *in vivo*. The localization at the plasma membrane of this intermediate state in the activation mechanism informs us about the site of Arf6 activation. It has recently been shown in epithelial cells that Arf6(T27N) localizes both to internal punctate structures and to adherens junctions (Palacios et al., 2001). In light of our results, the fraction of Arf6(T27N) found at the junctions might represent the fraction in complex with the endogenous exchange factor, leading to the inhibition of E-cadherin endocytosis (Palacios et al., 2002).

In order to determine the genuine cellular localization of the inactive GDP-bound form of Arf6, we designed a new mutant, Arf6(T44N), based on the three-dimensional structure of Arf6 in GDP- and GTP-bound conformations. Our approach proved to be correct because the T44N mutant has the same GDP-binding properties as the wild-type protein but displays a marked reduction in affinity for GTP. This mutant is essentially GDP bound when expressed in BHK cells, even when co-expressed with the GEF, demonstrating that the T44N mutation locked the protein in the GDP-bound form. Moreover, the absence of interaction between this T44N mutant and several Arf6 effectors (Fig. 5B and data not shown) demonstrate that this locked conformation is inactive. Arf6(T44N) distributes almost equally between cytosol and membrane fractions (Fig. 3). The membrane fraction of Arf6(T44N) is found in specific regions of the plasma membrane enriched in actin, PIP₂ and ezrin, an actin- and PIP₂-binding protein. The Arf6-specific exchange factor EFA6 localizes with Arf6 in these regions, suggesting that these microvillus-like structures of the plasma membrane are the sites of Arf6 activation. The fact that ARF6(T44N) is expressed in large excess of the endogenous EFA6 suggests the existence of a specific protein and/or lipid receptor(s) for Arf6-GDP. To date, beside the GEFs, $\beta\gamma$ subunits of trimeric G-proteins and β -arrestin are potential partners of Arf-GDP (Claing et al., 2001; Franco et al., 1995b; Galas et al., 1997). In light of the above, it would be interesting to look for a role of these two proteins as plasma membrane receptors for Arf6-GDP.

The localization of Arf6-GDP, Arf6-GTP and its putative GEFs EFA6 and Arno (Klarlund et al., 1997; Langille et al., 1999; Venkateswarlu et al., 1998) is more compatible with a role for Arf6 in cell surface endocytosis than in recycling from intracellular compartments. Nevertheless, recent IF studies looking at the intracellular accumulation of several molecules showed that Arf6 affects the recycling of receptors internalized by a clathrin-independent mechanism. In adipocytes, the translocation of the glucose transporter GLUT4 in response to endothelin has been proposed to be regulated by Arf6 (Lawrence and Birnbaum, 2001). The stimulated exocytosis of noradrenaline in permeabilized chromaffin cells and of exogenous growth hormone in PC12 cells seem to be controlled by the activation of Arf6 at the plasma membrane (Caumont et al., 2000). However, we believe that the localization of Arf6 and EFA6 precludes the possibility that Arf6 regulates the formation of recycling vesicles from an intracellular compartment destined to the plasma membrane. To explain how Arf6 could control the transport to the cell surface in such a wide variety of systems, we propose that Arf6

might also control the docking and/or fusion with the plasma membrane. This could be achieved by a modification in phospholipid composition of the plasma membrane as well as a reorganization of the underlying actin cytoskeleton.

We found a significant colocalization of Arf6-GDP with the Tfn-R at the plasma membrane but outside the area labelled for clathrin. As Arf6 is involved in Tfn-R endocytosis (D'Souza-Schorey et al., 1995), we would speculate that the GDP-GTP cycle of Arf6 is required for the recruitment of the Tfn-R into the clathrin-coated pits. In a similar manner, it has been proposed that the GTP hydrolysis by Arf1 is needed for the recruitment of the cargo into COPI-coated vesicles (Lanoix et al., 1999; Yang et al., 2002). Interestingly, a recent study on G-protein-coupled-receptor endocytosis suggested a role for Arf6 by interacting directly with the β -arrestin (Claing et al., 2001). This latter protein would promote Arf6 activation at the plasma membrane by recruiting Arf6-GDP and its GEF. Once activated, Arf6 would trigger clathrin translocation onto the membrane. Thus β -arrestin would act as a linker between the receptor and the recruitment of the coat mediated by Arf6 activation. β -Arrestin should be restricted to G-protein-coupled receptors. One could speculate that an equivalent protein will couple Arf6 activation to endocytosis of other groups of receptors.

In conclusion, we have demonstrated that the GDP-GTP cycle of Arf6 takes place at the plasma membrane, implying that Arf6 is essentially involved in the regulation of plasma-membrane-related processes. Identification of partners and molecular analysis in reconstituted model is now necessary to understand the multiple functions of Arf6 at the plasma membrane.

The authors are grateful to S. Bourgoin, T. Dubois, A. Galmiche, H. P. Hauri, V. Hsu and M. Martin for reagents. B. Antonny, M. Chabre, C. Favard, S. Paris, P. J. Peters and K. Singer are thanked for very stimulating discussions and helpful comments on this manuscript. This work was supported by CNRS institutional funding and a grant from the Ligue Nationale Française Contre le Cancer.

References

- Aikawa, Y. and Martin, T. F. (2003). ARF6 regulates a plasma membrane pool of phosphatidylinositol(4,5)bisphosphate required for regulated exocytosis. *J. Cell Biol.* **162**, 647-659.
- Altschuler, Y., Liu, S., Katz, L., Tang, K., Hardy, S., Brodsky, F., Apodaca, G. and Mostov, K. (1999). ADP-ribosylation factor 6 and endocytosis at the apical surface of Madin-Darby canine kidney cells. *J. Cell Biol.* **147**, 7-12.
- Barret, C., Roy, C., Montcourrier, P., Mangeat, P. and Niggli, V. (2000). Mutagenesis of the phosphatidylinositol 4,5-bisphosphate (PIP₂) binding site in the NH₂-terminal domain of ezrin correlates with its altered cellular distribution. *J. Cell Biol.* **151**, 1067-1080.
- Brown, H. A., Gutowski, S., Moomaw, C. R., Slaughter, C. and Sternweis, P. C. (1993). ADP-ribosylation factor, a small GTP-dependent regulatory protein, stimulates phospholipase D activity. *Cell* **75**, 1137-1144.
- Caumont, A. S., Vitale, N., Gensse, M., Galas, M. C., Casanova, J. E. and Bader, M. F. (2000). Identification of a plasma membrane-associated guanine nucleotide exchange factor for ARF6 in chromaffin cells. Possible role in the regulated exocytotic pathway. *J. Biol. Chem.* **275**, 15637-15644.
- Chavrier, P. and Franco, M. (2001). Expression, purification, and biochemical properties of EFA6, a Sec7 domain-containing guanine exchange factor for ADP-ribosylation factor 6 (ARF6). *Methods Enzymol.* **329**, 272-279.
- Chavrier, P. and Goud, B. (1999). The role of ARF and Rab GTPases in membrane transport. *Curr. Opin. Cell Biol.* **11**, 466-475.
- Claing, A., Chen, W., Miller, W. E., Vitale, N., Moss, J., Premont, R. T.

- and Lefkowitz, R. J. (2001). beta-Arrestin-mediated ADP-ribosylation factor 6 activation and beta 2-adrenergic receptor endocytosis. *J. Biol. Chem.* **276**, 42509-42513.
- Cockcroft, S., Thomas, G. M., Fensome, A., Geny, B., Cunningham, E., Gout, I., Hiles, I., Totty, N. F., Truong, O. and Hsuan, J. J. (1994). Phospholipase D: a downstream effector of ARF in granulocytes. *Science* **263**, 523-526.
- D'Souza-Schorey, C., Li, G., Colombo, M. I. and Stahl, P. D. (1995). A regulatory role for ARF6 in receptor-mediated endocytosis. *Science* **267**, 1175-1178.
- D'Souza-Schorey, C., van Donselaar, E., Hsu, V. W., Yang, C., Stahl, P. D. and Peters, P. J. (1998). ARF6 targets recycling vesicles to the plasma membrane: insights from an ultrastructural investigation. *J. Cell Biol.* **140**, 603-616.
- Derrien, V., Couillault, C., Franco, M., Martineau, S., Montcourrier, P., Houlgatte, R. and Chavrier, P. (2002). A conserved C-terminal domain of EFA6-family ARF6-guanine nucleotide exchange factors induces lengthening of microvilli-like membrane protrusions. *J. Cell Sci.* **115**, 2867-2879.
- Feig, L. A. (1999). Tools of the trade: use of dominant-inhibitory mutants of Ras-family GTPases. *Nat. Cell Biol.* **1**, E25-E27.
- Ferguson, K. M. and Higashijima, T. (1991). Preparation of guanine nucleotide-free G proteins. *Methods Enzymol.* **195**, 188-192.
- Franco, M., Boretto, J., Robineau, S., Monier, S., Goud, B., Chardin, P. and Chavrier, P. (1998). ARNO3, a Sec7-domain guanine nucleotide exchange factor for ADP ribosylation factor 1, is involved in the control of Golgi structure and function. *Proc. Natl. Acad. Sci. USA* **95**, 9926-9931.
- Franco, M., Chardin, P., Chabre, M. and Paris, S. (1995a). Myristoylation of ADP-ribosylation factor 1 facilitates nucleotide exchange at physiological Mg^{2+} levels. *J. Biol. Chem.* **270**, 1337-1341.
- Franco, M., Chardin, P., Chabre, M. and Paris, S. (1996). Myristoylation-facilitated binding of the G protein ARF1GDP to membrane phospholipids is required for its activation by a soluble nucleotide exchange factor. *J. Biol. Chem.* **271**, 1573-1578.
- Franco, M., Paris, S. and Chabre, M. (1995b). The small G-protein ARF1GDP binds to the Gt beta gamma subunit of transducin, but not to Gt alpha GDP-Gt beta gamma. *FEBS Lett.* **362**, 286-290.
- Franco, M., Peters, P. J., Boretto, J., van Donselaar, E., Neri, A., D'Souza-Schorey, C. and Chavrier, P. (1999). EFA6, a sec7 domain-containing exchange factor for ARF6, coordinates membrane recycling and actin cytoskeleton organization. *EMBO J.* **18**, 1480-1491.
- Galas, M. C., Helms, J. B., Vitale, N., Thiersé, D., Aunis, D. and Bader, M. F. (1997). Regulated exocytosis in chromaffin cell. A potential role for a secretory granule-associated AEF6 protein. *J. Biol. Chem.* **272**, 2788-2793.
- Garcia-Mata R., Gao, Y. S. and Sztul, E. (2002). Hassles with taking out the garbage: aggravating aggresomes. *Traffic* **3**, 388-396.
- Godi, A., Pertile, P., Meyers, R., Marra, P., Di Tullio, G., Iurisci, C., Luini, A., Corda, D. and De Matteis, M. A. (1999). ARF mediates recruitment of PtdIns-4-OH kinase-beta and stimulates synthesis of PtdIns(4,5)P₂ on the Golgi complex. *Nat. Cell Biol.* **1**, 280-287.
- Goldberg, J. (1998). Structural basis for activation of ARF GTPase: mechanisms of guanine nucleotide exchange and GTP-myristoyl switching. *Cell* **95**, 237-248.
- Gruenberg, J. (2001). The endocytic pathway: a mosaic of domains. *Nat. Rev. Mol. Cell Biol.* **2**, 721-730.
- Honda, A., Nogami, M., Yokozeki, T., Yamazaki, M., Nakamura, H., Watanabe, H., Kawamoto, K., Nakayama, K., Morris, A. J., Frohman, M. A. et al. (1999). Phosphatidylinositol 4-phosphate 5-kinase alpha is a downstream effector of the small G protein ARF6 in membrane ruffle formation. *Cell* **99**, 521-532.
- Johnston, J. A., Ward, C. L. and Kopito, R. R. (1998). Aggresomes: a cellular response to misfolded proteins. *J. Cell Biol.* **143**, 1883-1898.
- Kahn, R. A. and Gilman, A. G. (1986). The protein cofactor necessary for ADP-ribosylation of Gs by cholera toxin is itself a GTP binding protein. *J. Biol. Chem.* **261**, 7906-7911.
- Klarlund, J. K., Guilherme, A., Holik, J. J., Virbasius, J. V., Chawla, A. and Czech, M. P. (1997). Signaling by phosphoinositide-3,4,5-trisphosphate through proteins containing pleckstrin and Sec7 homology domains. *Science* **275**, 1927-1930.
- Krauss, M., Kinuta, M., Wenk, M. R., De Camilli, P., Takei, K. and Haucke, V. (2003). ARF6 stimulates clathrin/AP-2 recruitment to synaptic membranes by activating phosphatidylinositol phosphate kinase type Igamma. *J. Cell Biol.* **162**, 113-124.
- Langille, S. E., Patki, V., Klarlund, J. K., Buxton, J. M., Holik, J. J., Chawla, A., Corvera, S. and Czech, M. P. (1999). ADP-ribosylation factor 6 as a target of guanine nucleotide exchange factor GRP1. *J. Biol. Chem.* **274**, 27099-27104.
- Lanoix, J., Ouwendijk, J., Lin, C. C., Stark, A., Love, H. D., Ostermann, J. and Nilsson, T. (1999). GTP hydrolysis by Arf-1 mediates sorting and concentration of Golgi resident enzymes into functional COP I vesicles. *EMBO J.* **18**, 4935-4948.
- Lawrence, J. T. and Birnbaum, M. J. (2001). ADP-ribosylation factor 6 delineates separate pathways used by endothelin 1 and insulin for stimulating glucose uptake in 3T3-L1 adipocytes. *Mol. Cell Biol.* **21**, 5276-5285.
- Lerosey, I., Chardin, P., de Gunzburg, J. and Tavittian, A. (1991). The product of the *rap2* gene, member of the Ras superfamily. Biochemical characterization and site-directed mutagenesis. *J. Biol. Chem.* **266**, 4315-4321.
- Macia, E., Chabre, M. and Franco, M. (2001). Specificities for the small G proteins ARF1 and ARF6 of the guanine nucleotide exchange factors ARNO and EFA6. *J. Biol. Chem.* **276**, 24925-24930.
- Macia, E., Paris, S. and Chabre, M. (2000). Binding of the PH and polybasic C-terminal domains of ARNO to phosphoinositides and to acidic lipids. *Biochemistry* **39**, 5893-5901.
- Massenburg, D., Han, J. S., Liyanage, M., Patton, W. A., Rhee, S. G., Moss, J. and Vaughan, M. (1994). Activation of rat brain phospholipase D by ADP-ribosylation factors 1, 5, and 6: separation of ADP-ribosylation factor-dependent and oleate-dependent enzymes. *Proc. Natl. Acad. Sci. USA* **91**, 11718-11722.
- Menetrey, J., Macia, E., Pasqualato, S., Franco, M. and Cherfils, J. (2000). Structure of Arf6-GDP suggests a basis for guanine nucleotide exchange factors specificity. *Nat. Struct. Biol.* **7**, 466-469.
- Niedergang, F., Colucci-Guyon, E., Dubois, T., Raposo, G. and Chavrier, P. (2003). ADP ribosylation factor 6 is activated and controls membrane delivery during phagocytosis in macrophages. *J. Cell Biol.* **161**, 1143-1150.
- Niggli, V., Andreoli, C., Roy, C. and Mangeat, P. (1995). Identification of a phosphatidylinositol-4,5-bisphosphate-binding domain in the N-terminal region of ezrin. *FEBS Lett.* **376**, 172-176.
- Palacios, F., Price, L., Schweitzer, J., Collard, J. G. and D'Souza-Schorey, C. (2001). An essential role for ARF6-regulated membrane traffic in adherens junction turnover and epithelial cell migration. *EMBO J.* **20**, 4973-4986.
- Palacios, F., Schweitzer, J. K., Boshans, R. L. and D'Souza-Schorey, C. (2002). ARF6-GTP recruits Nm23-H1 to facilitate dynamin-mediated endocytosis during adherens junctions disassembly. *Nat. Cell Biol.* **12**, 929-936.
- Paris, S., Beraud-Dufour, S., Robineau, S., Bigay, J., Antonny, B., Chabre, M. and Chardin, P. (1997). Role of protein-phospholipid interactions in the activation of ARF1 by the guanine nucleotide exchange factor Arno. *J. Biol. Chem.* **272**, 22221-22226.
- Pasqualato, S., Menetrey, J., Franco, M. and Cherfils, J. (2001). The structural GDP/GTP cycle of human Arf6. *EMBO Rep.* **2**, 234-238.
- Pasqualato, S., Renault, L. and Cherfils, J. (2002). Arf, Arl, Arp and Sar proteins: a family of GTP-binding proteins with a structural device for 'front-back' communication. *EMBO Rep.* **3**, 1035-1041.
- Peters, P. J., Hsu, V. W., Ooi, C. E., Finazzi, D., Teal, S. B., Oorschot, V., Donaldson, J. G. and Klausner, R. D. (1995). Overexpression of wild-type and mutant ARF1 and ARF6: distinct perturbations of nonoverlapping membrane compartments. *J. Cell Biol.* **128**, 1003-1017.
- Radhakrishna, H. and Donaldson, J. G. (1997). ADP-ribosylation factor 6 regulates a novel plasma membrane recycling pathway. *J. Cell Biol.* **139**, 49-61.
- Radhakrishna, H., Klausner, R. D. and Donaldson, J. G. (1996). Aluminum fluoride stimulates surface protrusions in cells overexpressing the ARF6 GTPase. *J. Cell Biol.* **134**, 935-947.
- Stammes, M. A. and Rothman, J. E. (1993). The binding of AP-1 clathrin adaptor particles to Golgi membranes requires ADP-ribosylation factor, a small GTP-binding protein. *Cell* **73**, 999-1005.
- Szoka, F., Jr and Papahadjopoulos, D. (1978). Procedure for preparation of liposomes with large internal aqueous space and high capture by reverse-phase evaporation. *Proc. Natl. Acad. Sci. USA* **75**, 4194-4198.
- Venkateswarlu, K., Oatley, P. B., Tavare, J. M. and Cullen, P. J. (1998). Insulin-dependent translocation of ARNO to the plasma membrane of adipocytes requires phosphatidylinositol 3-kinase. *Curr. Biol.* **8**, 463-466.
- Yang, J. S., Lee, S. Y., Gao, M., Bourgoin, S., Randazzo, P. A., Premont, R. T. and Hsu, V. W. (2002). ARFGAP1 promotes the formation of COPI vesicles, suggesting function as a component of the coat. *J. Cell Biol.* **159**, 69-78.